ELSEVIER

Thin Solid Films 342 (1999) 74–82

thin solid films

Influence of oxygen and nitrogen on the growth of hot-filament chemical vapor deposited diamond films

Z. Yu*, U. Karlsson, A. Flodström

Materials Physics, Department of Physics, Royal Institute of Technology, Teknikringen 14, S-100 44 Stockholm, Sweden

Received 31 January 1998; accepted 28 August 1998

Abstract

The effect of incorporating oxygen and nitrogen into the feed gases on the texture and surface morphology of diamond film synthesized by hot filament chemical vapor deposition (HFCVD) is investigated. The reactant gas composition is determined by the gas flow rates. At a constant flow rate of hydrogen (33 sccm) and methane (0.68 sccm), the oxygen and nitrogen were varied in the O/(O + C) ratio from 0.05 to 0.43 and in the N/(N + C) ratio from 0.15 to 0.60. The films were grown under a constant pressure (20 Torr) and a constant substrate temperature (800°C). Clearly nitrogen in the reactant gases has a distinct tendency to promote the ⟨100⟩ texture and the corresponding {100} morphology, whereas oxygen promotes the development of ⟨111⟩ texture and {111} morphology. According to the Wulff theorem ($\Gamma = d_{100}/d_{111} = \gamma_{100}/\gamma_{111}$) and the evolutionary selection of crystallites and the surface configurations of diamond, the results reveal that during growth nitrogen plays a critical role in activating the C_D–H surface site and consequently increases the surface free energy γ_{111}, of the {111} surface. In contrast, oxygen activates the C_D=H_2 surface site and increases the surface free energy γ_{100}, of the{100} surface. These results indicate that the texture and the surface morphology of polycrystalline diamond film can be completely controlled by the reactant gas composition.

Keywords: Chemical vapour deposition; Diamond films

1. Introduction

It is important to control the microstructure of chemical vapor deposited (CVD) diamond films in order to achieve the theoretical potential of their application [1]. Highly oriented (111) diamond films are potentially useful for field-induced electron emission in display devices, since (111) planes of diamond exhibit negative electron affinity [2]. A strong correlation between surface morphology and electric conductivity was found by Jin and Moustakas [3].

The ratio of the ⟨100⟩ to the ⟨111⟩ growth rates, $\Gamma = \nu_{100}/\nu_{111}$, where ν_{100} and ν_{111} denote respectively the growth rates in ⟨100⟩ and ⟨111⟩ orientations, is conventionally considered to relate to the {111}/{100} surface area ratio on microcrystals [4–6] and to texture formation in polycrystalline films [1,7–12]. From the growth geometry of a crystal and thermodynamics [13–15], one finds that the octahedron crystal form with {111} facets corresponds to $\Gamma \geq \sqrt{3}$ and that the rhombic dodecahedron with {110} facets corresponds to $\Gamma = 2/\sqrt{3}$, whereas, the cube with {100} facets requires $\Gamma \leq 1/\sqrt{3}$.

It is well known that the textured growth of CVD diamond films is improved by adjusting deposition parameters such as the gas composition [1,7,10,16–21], the temperature of the substrate [8] and filament [7,9,16,19,20, 22–25], and the ambient pressure [5]. A method for {111} oriented diamond film synthesis has been developed using controlled seeding of micro-sized diamond particles by electrophoresis [2]. Both oxygen and nitrogen are considered to be critically important for modifying the surface morphology and growth kinetics. The effects of concentrations of oxygen [1,6,26] and nitrogen [10,16] in the reactant gases have been widely investigated and they have been shown to modify Γ dramatically. Rawles et al. [1] report that Γ changed from 1.27 for growth without oxygen to 0.75 for growth with 0.14% oxygen. It was found that the growth mode of CVD diamond changed from {111} to {100} when the nitrogen in the gas phase was increased from N/C = 0.1% to 10% [19]. Locher et al. [12], however, showed that a diamond film synthesized by microwave plasma-assisted CVD with only 60 ppm nitrogen admixed in 1.5% CH_4 of reactant gases, had a complete {100} facet-terminated morphology.

There is a clear need for systematic studies on the effect on CVD diamond growth behavior of incorporating both

* Corresponding author. Tel.: + 46-8-790-7391; fax.: + 46-8-249-131; *E-mail address:* ming@matphys.kth.se (Z. Yu)

0040-6090/99/$ - see front matter
PII: S0040-6090(98)01352-2

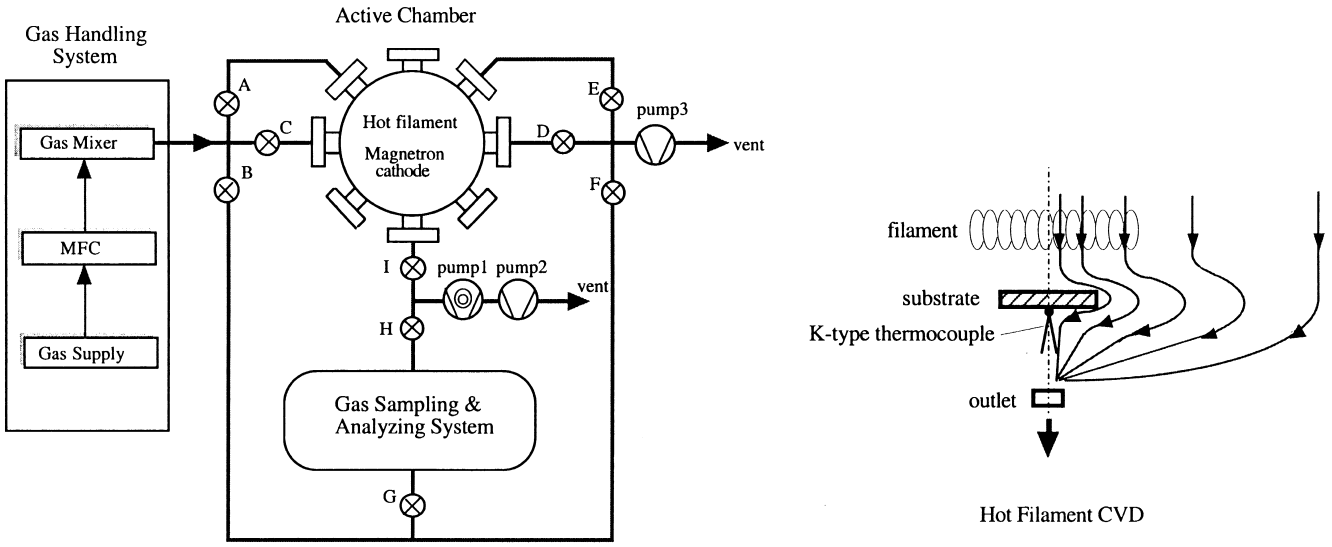

Fig. 1. Schematic drawing of the deposition system.

oxygen and nitrogen into the reactant gases. In the work presented in this paper, the influence of oxygen and nitrogen on growth behavior of CVD diamond films is investigated and a mechanism for the influence is proposed employing an atomistic model.

2. Experimental

The films were synthesized by the method of hot filament assisted chemical vapor deposition (HFCVD) in a vapor deposition system especially designed for diamond deposition. It consists of a gas handling system, a reactor and a gas sampling and analyzing system, as shown in Fig. 1. The reactor is a stainless steel chamber with an inner diameter of 300 mm to which are fitted various electrical, gas and liquid feedthroughs, as well as a magnetron cathode. A linear motion feedthrough allowed in situ control of the filament–substrate distance. By changing the distance the substrate temperature can be adjusted. In order to achieve similar heating histories for each sample, a new tungsten filament (diameter 0.38 mm) coiled with 14 turns (inner diameter 1 mm) was used. The temperatures of the tungsten filament and the substrate measured by an optical pyrometer and a K-type thermocouple were set at 2000 and 800°C, respectively. The base pressure is less than 1×10^{-6} Torr maintained by a turbomolecular pump. The deposition pressure is monitored and controlled using a manometer coupled to valve E on the vacuum line. The gas analyzer is a quadrupole mass spectrometer (Balzers QMS200). Gas flow can be sampled at the inlet for feed gases and at the outlet for exhaust gases into the QMS chamber to be analyzed. Table 1 shows parameters which are expected to be kept constant

Table 1
Parameters of HFCVD diamond films

Substrate	p-type Si(100) roughened with 1 μm diamond grit
Hydrogen flow rate (sccm)	33
Methane flow rate (sccm)	0.68
Filament temperature T_f (°C)	2100 ± 50
Substrate temperature T_s (°C)	750 ± 10
Total pressure (Torr)	20 ± 0.5
Deposition time (h)	20

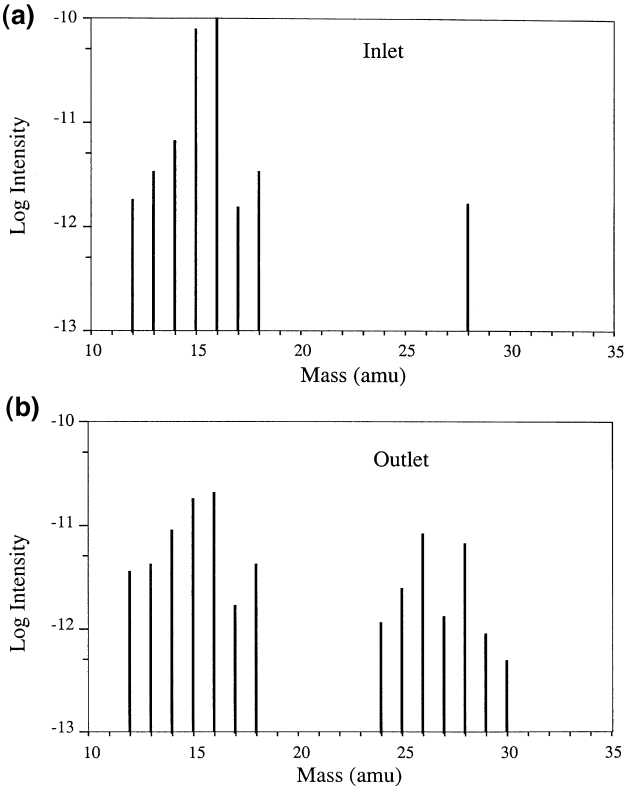

Fig. 2. Mass spectra of inlet and outlet gas asmples.

Table 2
The thickness and relative XRD intensity of diamond films deposited at various gas compositions

Sample	O/(O + C)	N/(N + C)	Film thickness (μm)	Relative XRD intensity {111}	{220}	{311}	{400}
Powder				100	25	16	8
a1	0	0	25	100	99	11	4
a2	0	0.15	20	100	16	14	38
a3	0	0.60	26	100	7	8	33
b1	0.06	0	25	100	9	8	–
b2	0.06	0.15	36	100	20	9	39
b3	0.06	0.60	29	100	17	10	161
c1	0.43	0	9	100	26	5	3
c2	0.43	0.15	11	100	26	10	3
c3	0.43	0.60	12	100	27	9	–

for each sample. The chamber was evacuated to less than 10^{-2} Torr prior to the introduction of the feed gases. The compositions of the reactant gases, H_2, CH_4, O_2 and N_2, were adjusted by their gas flow rates. The flow rate of CH_4 was set at 0.68 sccm with 33 sccm hydrogen, while those of oxygen and nitrogen were varied from 0.02 to 0.26 sccm and from 0.06 to 0.49 sccm, respectively. The substrate used for sampling was a 8×15 mm^2 (100) silicon wafer roughened with 1 μm diamond grit. The microstructure and quality of the films were investigated by scanning electron microscopy (SEM) and X-ray diffraction (XRD).

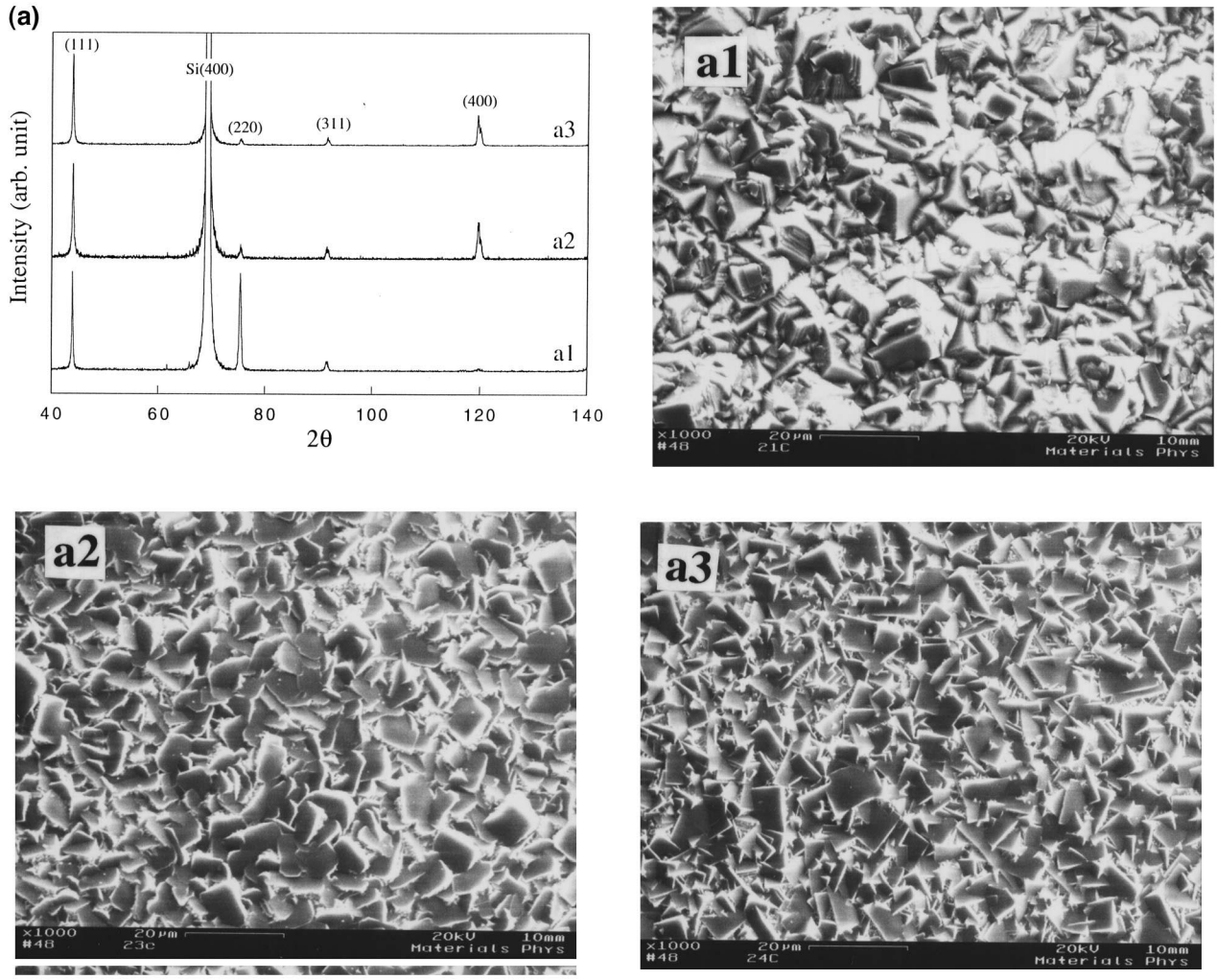

Fig. 3. X-ray diffraction patterns and corresponding SEM images of diamond films synthesized at the composition points a1, a2 and a3.

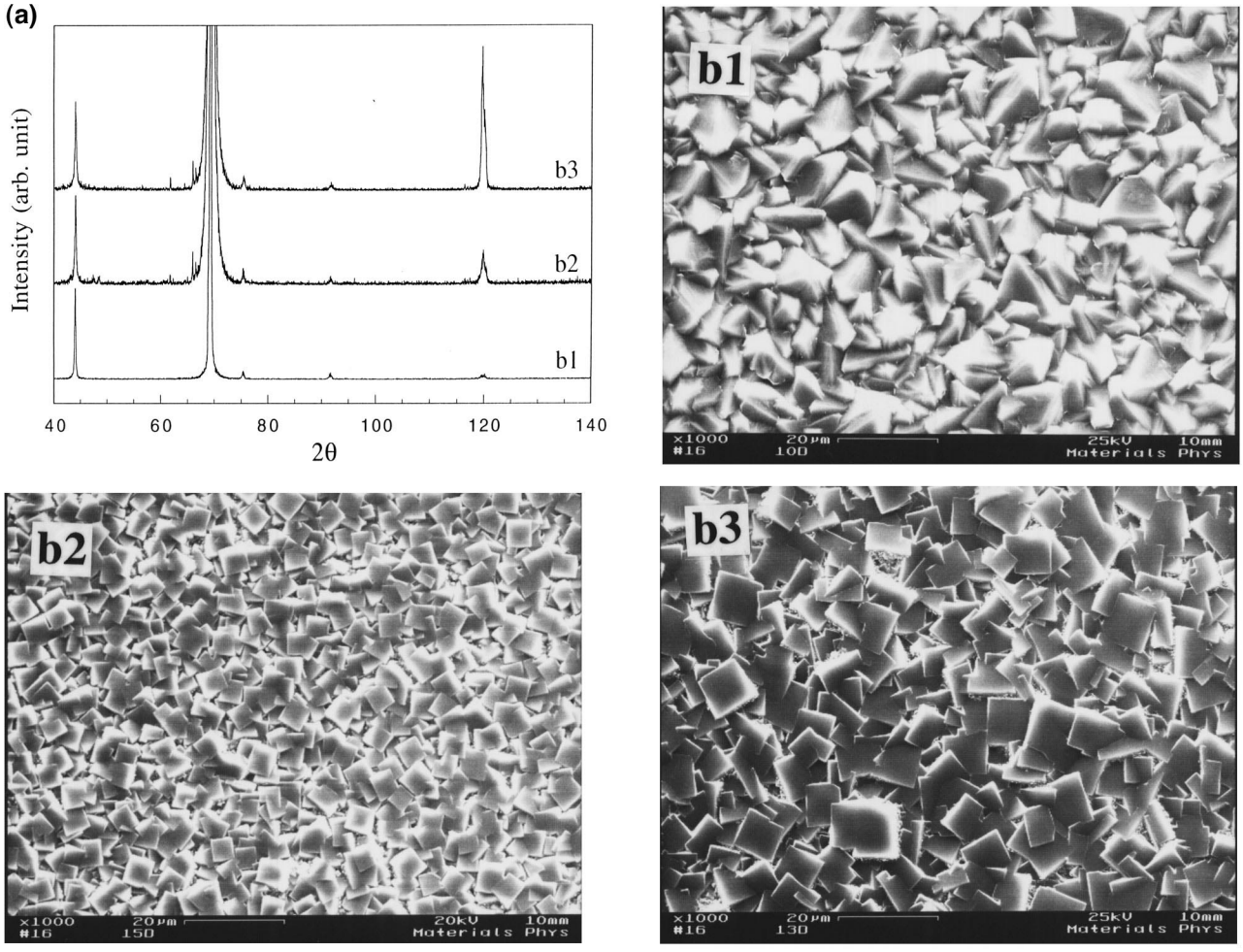

Fig. 4. X-ray diffraction patterns and corresponding SEM images of diamond films synthesized at the composition points b1, b2 and b3.

3. Results

Fig. 2 shows the raw mass spectra of both inlet and outlet gases under standard conditions (a1). The mass spectrometer had a range of 1–100 amu, but no hydrocarbons with amu >44 were detected. Comparing with the peaks of the inlet gas, a peak of 30 amu in the gas sample from the outlet reveals that NO or NO_2 was formed during the HFCVD diamond. The formation of NO or NO_2 uses nitrogen and oxygen and consequently modifies the concentrations of nitrogen and oxygen from the original values.

Table 2 shows the film thickness and the relative X-ray diffraction intensities of the diamond films under various composition points. Growth rates of diamond of about 0.55 and 1.0 μm/h were observed with and without oxygen, respectively. The decrease in the growth rate of CVD diamond with increasing oxygen concentration agrees with the results of Rawles et al. [1].

In X-ray powder diffraction, only crystallographic planes parallel to the deposition plane of the film contribute to the diffraction pattern, so that a comparison of the diffraction intensities of planes in a film with those of the same planes in an isotropic powder sample allows a qualitative determination of the texture in the film parallel to the deposition plane [12,16,27]. In Table 2 it should be noted that the data obtained at each composition point on different occasions are in agreement with each other.

Fig. 3a,b show the XRD patterns of different films and their corresponding surface morphologies with increasing concentration of nitrogen in the feed gas with the oxygen concentration equal to zero. When both oxygen and nitrogen were absent, i.e. at the composition point a1 given in Table 2, the film shows a ⟨110⟩ texture since $I_{220}/I_{111} = 0.99$, compared with 0.25 in standard powder samples. The relative XRD intensities, I_{400}/I_{111}, were 0.38 and 0.33 when the N/(N + C) ratio was set at 0.15 and 0.60 (i.e. at composition points a2 and a3), respectively. The relative intensities are larger than that of the isotropic sample, 0.08, indicating a ⟨100⟩ texture of the films.

When the O/(O + C) ratio was 0.05, the relative intensity of I_{400}/I_{111} increased considerably from 0 to 1.61 when the N/(N + C) ratio increased from 0 to 0.60 (i.e. composition points b1, b2 and b3). No obvious (400) peak of the film b1

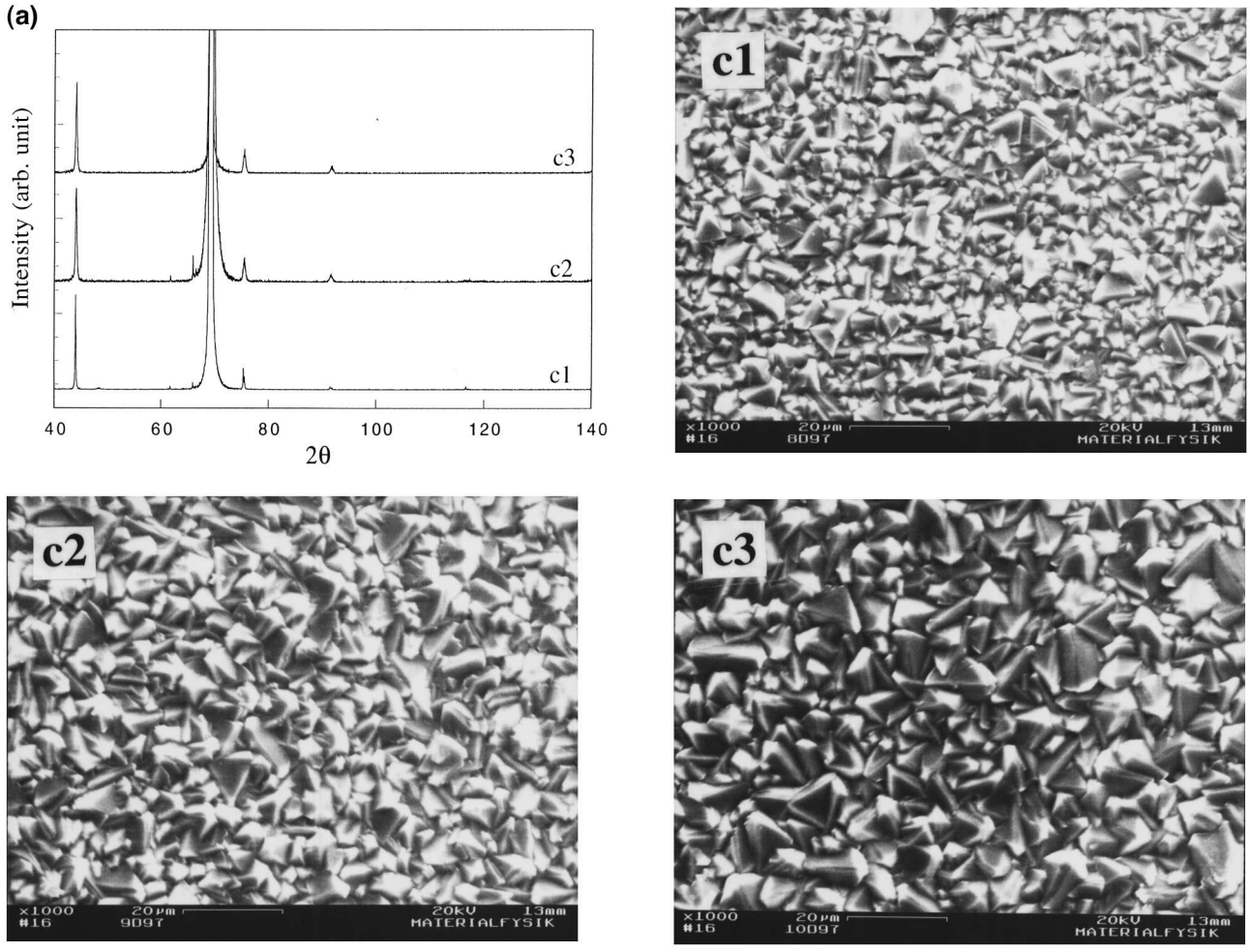

Fig. 5. X-ray diffraction patterns and corresponding SEM images of diamond films synthesized at the composition points c1, c2 and c3.

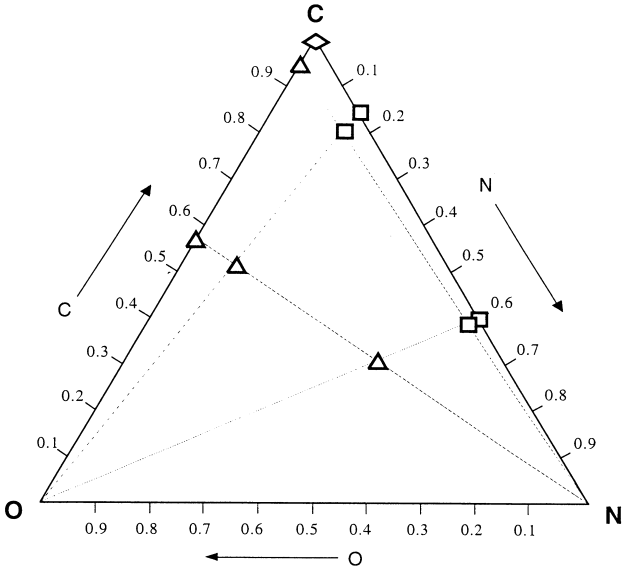

Fig. 6. Atomic C–O–N phase diagram with surface morphologies (or textures) of HFCVD diamond obtained at fixed parameters $P = 30$ Torr, $T_s = 750$°C, $H_2 = 33$ sccm and $CH_4 = 0.68$ sccm. Triangles, squares and rhomboids represent dominant growth of {111}, {100} and {110} respectively.

indicates that it was grown in ⟨111⟩ texture, whereas the relative intensity of I_{400}/I_{111} of sample b3 was 1.61 which is much higher than that of the standard powder sample, revealing that the films are ⟨100⟩ textured. Fig. 4a,b show the SEM morphologies and the XRD patterns of these samples. Both SEM and XRD show that at a ratio of O/(O + C) of 0.05, nitrogen in the feed induced a sharp transition of texture from ⟨111⟩ to ⟨100⟩ or morphology from {111} to {100}.

With a further increase of the oxygen concentration to a O/(O + C) ratio of 0.43, the films show significant {111} morphologies in SEM photographs and no obvious (400) peak in the XRD pattern, as shown in Fig. 5a,b. It is also evident in Fig. 5 that there was no change in the morphology and texture of the films when the nitrogen concentration was increased to a N/(N + C) ratio of 0.60. A further increase in the nitrogen concentration, however, led to a deterioration in the film quality.

In general, the influence of oxygen and nitrogen on the growth habit of HFCVD diamond may be approximately shown in a C–O–N phase diagram (Fig. 6). Oxygen and nitrogen seem to have threshold concentrations at which

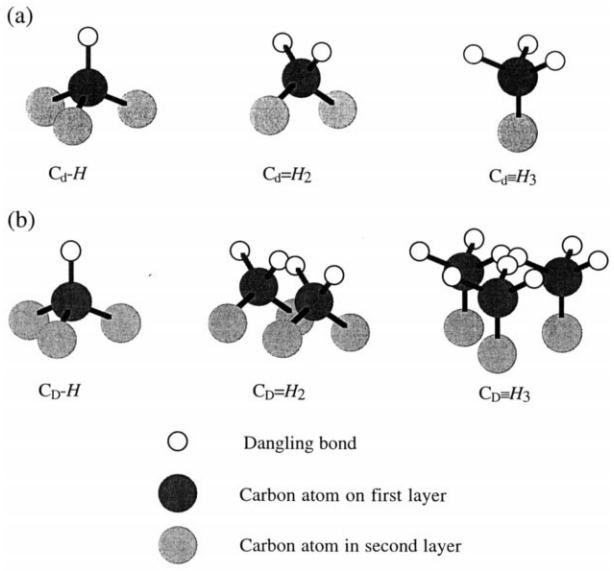

Fig. 7. (a) Three configurations of the surface atom of diamond bonded with dangling bond(s): C_d–H, C_d=H_2 and C_d≡H_3, where C_d denotes an individual carbon atom at the surface of diamond and H a dangling bond. (b) Three kinds of surface site consist of surface carbon atoms bonded with H: C_D–H, C_D=H_2 and C_D≡H_3, where C_D refers to a diamond surface but not an individual surface carbon atom. Three individual surface atoms of C_d≡H_3 contribute respectively one-third to the C_D≡H_3 site, two individual surface atoms of C_d=H_2 contribute respectively one-half to the C_D=H_2 site and the surface atom C_d–H itself is the C_D–H site.

the film morphology transfers from {110} to {111} and {100} respectively.

4. Discussion

In the present case, the content of hydrogen was always greater than 95.8%, and the contents of oxygen and nitrogen were less than 0.76% and 1.42%, respectively. The thermal conductivity of hydrogen is evidently much greater than that of both oxygen and nitrogen [28]. It is therefore reasonable to ignore the effect of the gas composition on thermal conductivity in the following discussion.

The influence of N_2 and O_2 in the feed on the morphology of polycrystalline CVD diamond films has been widely studied [1,3,10,16,29]. So far, the mechanism by which the nitrogen and oxygen admixture influences the texture and the morphology of the films is not completely understood. The current understanding is that the change in morphology is explained in terms of a variation of the growth parameter Γ [9,10,30,31]. However, it should be noted that strictly speaking Γ is not a ratio of growth rates but a ratio of distances $\Gamma = d_{100}/d_{111}$, where d_{hkl} is the distance from Wulff point to the surface (hkl) [5,32-34]. In essence it is a ratio of the surface free energies, i.e. $\Gamma = \gamma_{100}/\gamma_{111}$, where γ_{hkl} is the surface free energy [5,30,33,34].

It is known that the ideal surface free energy (SFE) of a crystal, which is a function of both the bond energy and the surface configuration of the crystal [15], determines the equilibrium form of the crystal [5,15]. However, during crystal growth, the surface free energy is not only dependent on the bond energy and the surface configuration but also on surface reactions which occur during the growth [13]. It is called the as-growing surface free energy (AGSFE). It is therefore evident that the AGSFE is different from the SFE, and thus that growth forms of a crystal differ from the equilibrium form because the growth form is determined by the AGSFE [13,14,16,17].

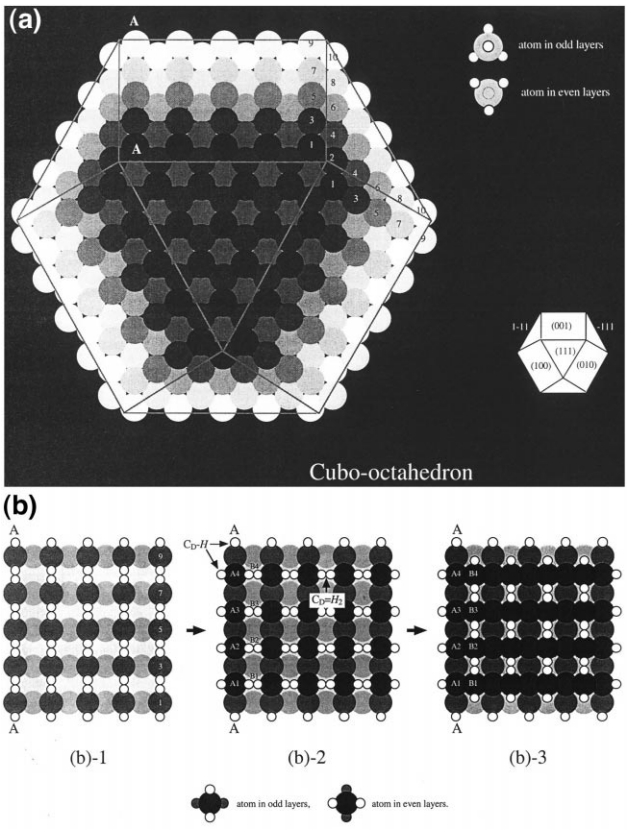

Fig. 8. (a) Sterically schematic drawing of cubo-octahedron by stacking {111} planes parallel to the plane of the paper. The sphere represents a carbon atom and its size is proportional to the size of carbon atoms in the actual lattice. Lighter color atoms lie in deeper layers and the numbers on the spheres represent the sequence of layers of the {111} plane. Dangling bonds are omitted for clarity. Two configurations of carbon atoms due to bond orientation are inserted. From the two configurations of atoms in odd and even layers respectively, it is found that the {100} and {111} surfaces of a cubo-octahedron are covered with the C_D=H_2 and C_D–H sites respectively. The atoms on the edge of AA belong to both the (1 − 11) and the (001) surfaces. (b) Occupation of the C_D=H_2 sites on the (001) surface. When the C_D=H_2 sites on AA are occupied, adatoms on AA (A1, A2, A3 and A4) will produce both the C_D=H_2 sites on (001) and the C_D–H sites on (1 − 11) as shown in (b)-2, implying that they belong to these two surfaces. Further occupation of the C_D=H_2 sites (e.g. B1,B2, B3 and B4) makes the atoms on AA produce only the C_D–H sites on (1 − 11), as shown in (b)-3, implying that they belong to the (1 − 11) surface only. Therefore if the C_D=H_2 sites are preferentially occupied by adatoms, the number of C_D=H_2 sites must decrease and the number of C_D–H sites must increase, so that {111} is preferential for growth.

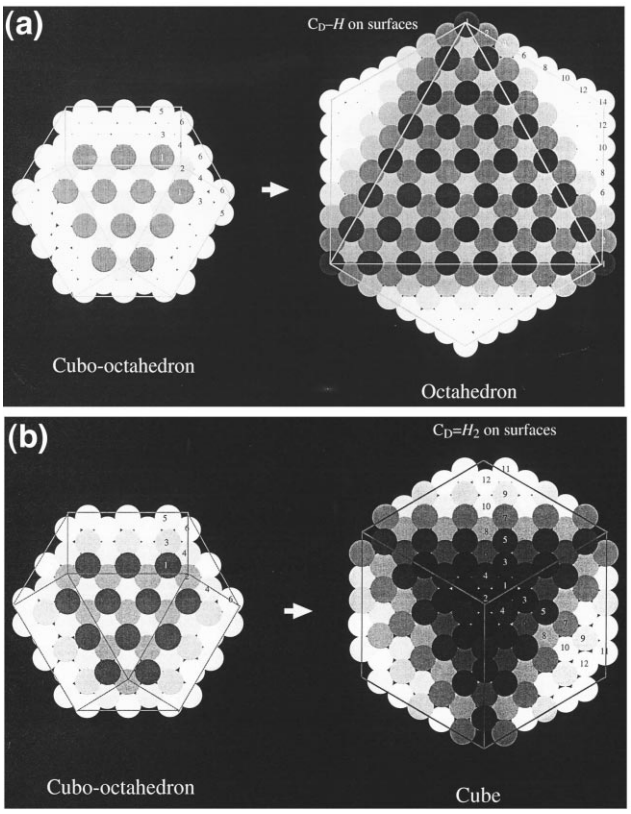

Fig. 9. (a) When the $C_D{=}H_2$ site is preferentially occupied rather than the C_D–H site, the number of $C_D{=}H_2$ sites will decrease as growth proceeds because of the atomic structure of diamond. Otherwise, the number of C_D–H sites increases. Consequently, {111} surfaces become evolutionary and {100} surfaces degenerative. As a result of the growth, {111} are dominant surfaces which are covered with C_D–H sites and the crystal appears in the form of an octahedron. For simplicity, the condition that $\Gamma = 2\sqrt{3}$ is taken into account in the picture. (b) When the C_D–H site is preferentially occupied rather than the $C_D{=}H_2$ site, the number of C_D–H sites will decrease during growth. {100} is then dominant in surfaces which are covered with the $C_D{=}H_2$ sites and the crystal appears in the form of a cube. In this case, $\Gamma = (2\sqrt{3})^{-1}$.

Crystal growth is essentially a process replacing existing surface sites and consequentially producing new ones by adatoms. When an adatom lands (condenses) on a surface site, bond(s) will be generated and simultaneously the attachment energy will be released. The attachment energy is equal to the energy of the formed bond(s) which can be substituted for the surface free energy to determine the growth morphology of the crystal [35–38]. It is known that the occupation velocity of the site increases with increasing attachment energy [35]. Therefore, one finds that a high energy site is occupied preferentially if the site energy is defined as the attachment energy.

The surface site is naturally coincident with a lattice point. Thermodynamically, an activated surface site consists of a surface atom and corresponding dangling bond(s) [39,40]. In the tetrahedral configuration of carbon, there are only three possible ways of bonding a surface atom (C_d) with dangling bond(s) (H): C_d–H, $C_d{=}H_2$ and $C_d{\equiv}H_3$. Fig. 7a shows these three ways schematically. Hence diamond surfaces have to be terminated by H in one, two or three ways, and consequently produce three kinds of surface sites, C_D–H, $C_D{=}H_2$ and $C_D{\equiv}H_3$, as shown in Fig. 7b (where C_D refers to the diamond surface but not an individual surface carbon atom). For example, flat (111) surface can be terminated by C_d–H or by $C_d{\equiv}H_3$. Fig. 8a illustrates a perspective view of the cubo-octahedron with respect to the atomic stacking of diamond (111) planes. It is evident in this illustration that the flat surfaces of {100} and {111} are covered with the $C_D{=}H_2$ and C_D–H sites respectively. Similarly the flat surface of {110} is covered with the C_D–H site.

During the growth of diamond crystal, if one kind of site is energetically preferentially occupied, the crystal will be covered less and less with this kind of site. For example, if the $C_D{=}H_2$ site is preferentially occupied rather than the C_D–H site, as growth proceeds the number of $C_D{=}H_2$ sites will become less and less and the number of C_D–H sites will increase due to the configuration of diamond, as shown in Fig. 8b. Consequently, the {111} surfaces will be evolutionary and the {100} surfaces will be degenerative. Finally, the {111} will become dominant and the crystal will have the form of an octahedron as shown in Fig. 9a. In contrast, when the C_D–H site is preferentially occupied rather than the $C_D{=}H_2$ site, the {100} surfaces will be dominant (Fig. 9b). Therefore, it is qualitatively concluded that the growth of the diamond crystal is naturally determined by the property of the sites: when $C_D{=}H_2$ is preferentially occupied the {111} is favorable, whereas when C_D–H is preferentially occupied the {100} is favorable.

Naturally, the $C_D{=}H_2$ site is more easily occupied by adatoms than C_D–H, since it has twice the energy of the C_D–H site, which means that {111} facets are dominant. It is demonstrated that the equilibrium form of diamond is octahedron covered with {111} surfaces [15]. However, the actual morphology of the CVD diamond films deviates from the ideal equilibrium surface. The deviation of the morphologies is due to the AGSFE which differs from the SFE by modifying the site energies via surface reactions. In a future paper the relation of the AGSFE and the site energies will be discussed.

Recent experimental investigations on diamond surfaces reveal that oxygen restores preferentially the reconstructed (100) surface of diamond [41] and that nitrogen prefers incorporation into the (111) growth sector [42]. We therefore propose a mechanism to explain the influence of nitrogen and oxygen on the growth habit of CVD diamond: nitrogen and oxygen activate the sites of C_D–H and $C_D{=}H_2$ respectively. In other words, nitrogen and oxygen increase the site energies of C_d–H and $C_d{=}H_2$ respectively. So that nitrogen decreases Γ and oxygen increases Γ. Therefore, nitrogen makes the {100} facets energetically preferential for growth and oxygen does the same to {111} facets. Another possibility of increasing {111} by oxygen is that oxygen may react with nitrogen in the gas

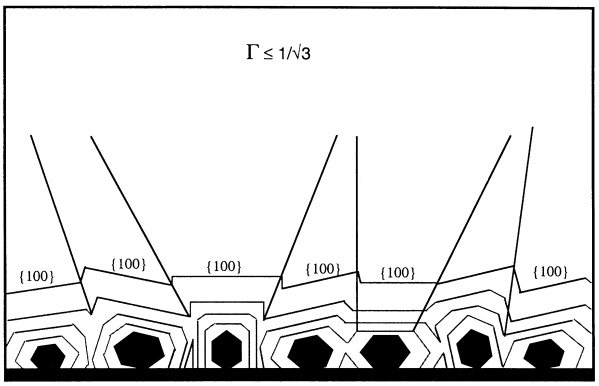

Fig. 10. The schematic growth of a polycrystalline diamond film, viewed from the side, from randomly oriented cubo-octahedron nuclei. For simplicity, only the crystals whose (100) planes are perpendicular to the plane of the paper are shown in the figure. In a real layer, the situation is somewhat more complicated; nevertheless the same principle applies.

phase to decrease the concentration of nitrogen, so that the effective influence of nitrogen is weakened.

When $\Gamma \leq 1/\sqrt{3}$, the {100} facets are dominant for individual grains of diamond. For the texturing growth of film, according to the evolutionary selection of crystallites proposed by van der Drift [43], after a long period of growth, only crystals which have one of their {100} facets perpendicular to the growth direction of the film will survive, whereas other particles with {100} facets which deviate from the growth direction are gradually buried. This growth will produce a ⟨100⟩ texture accompanied by a {100} morphology. Fig. 10 shows schematically a polycrystalline film grown from randomly oriented cubo-octahedron nuclei when $\Gamma \leq 1/\sqrt{3}$. Otherwise, when $\Gamma \geq \sqrt{3}$, only crystals having a {111} facet perpendicular to the growth direction of the film will survive, resulting in a ⟨111⟩ texture and {111} morphology.

It is known that the parameter Γ decreases from $\sqrt{3}$ to $1/\sqrt{3}$ (corresponding to a facet change from {111} to {100}) as the concentration of nitrogen increases [12,19]. If it is assumed that the change in Γ is proportional to the concentration of nitrogen, there must be a nitrogen concentration giving $\Gamma = 2/\sqrt{3}$ which is the thermodynamic condition for dominant {110} facets. Therefore, the ⟨110⟩ texture of diamond films synthesized at the composition point a1 may be due to nitrogen from a leakage. Since the production of NO or NO_2 in the gas phase uses nitrogen and oxygen, the actual influence of nitrogen and oxygen on the C_D–H and $C_D{=}H_2$ sites is respectively proportional to the effective concentrations of nitrogen and oxygen after the formation of NO or NO_2.

5. Conclusion

The influence of nitrogen and oxygen in the reactant gas on the texture and morphology of HFCVD diamond films has been investigated. When $P = 20$ Torr, $T_s = 750$°C, $H_2 = 33$ sccm and $CH_4 = 0.54$– 0.68 sccm, the relation between the growth morphologies (textures) and the composition is shown in the phase diagram (Fig. 6). When O/(O + C) $\leq$ 0.05, the growth behavior of the diamond film tends to form the ⟨100⟩ texture as the concentration of nitrogen increases. At O/(O + C) = 0.43, however, the ⟨111⟩ texture is dominant and is not affected by an increase in nitrogen concentration up to N/(N + C) = 0.60. The results indicate that the growth mode of HFCVD diamond films can be completely controlled by gas composition.

The results provide information leading to an understanding of the mechanism of HFCVD diamond. The role of nitrogen in CVD diamond is to activate the C_D–H site and consequently to increase the surface free energy, γ_{111}, of the {111} surface. Otherwise, oxygen may increase the $C_D{=}H_2$ site energy, making γ_{100} higher. Therefore, since $\Gamma = d_{100}/d_{111} = \gamma_{100}/\gamma_{111}$ and the evolutionary selection of crystallites, the ⟨100⟩ and ⟨111⟩ textures and the corresponding {100} and {111} morphologies of HFCVD diamond films are improved with increasing concentration of nitrogen and oxygen, respectively.

Acknowledgements

The authors would like to acknowledge the financial support of Swedish Research Council for Engineering Sciences.

References

[1] R. Rawles, W. Morris, M. D'Evelyn, Appl. Phys. Lett. 69 (1996) 4032.
[2] R. Singh, D. Lee, Appl. Phys. Lett. 70 (1997) 1542.
[3] S. Jin, T. Moustakas, Appl. Phys. Lett. 63 (1993) 2354.
[4] A. Wells, Philos. Mag. 37 (1946) 605.
[5] Z. Yu, A. Flodstrom, Diamond Relat. Mater. 6 (1997) 81.
[6] Y.-J. Baik, K. Y. Eun, Thin Solid Films 214 (1992) 123.
[7] B. Spitsyn, L. Bouilov, B. Derjaguin, J. Cryst. Growth 52 (1981) 219.
[8] R. Meilunas, M.S. Wong, K.C. Sheng, R.P.H. Chang, Appl. Phys. Lett. 54 (1989) 2204.
[9] C. Wild, N. Herres, P. Koidl, J. Appl. Phys. 68 (1990) 973.
[10] C. Chu, R. Hauge, J. Margrave, M. D'Evelyn, Appl. Phys. Lett. 61 (1992) 1393.
[11] C. Wild, P. Koidl, W. Muller-Sebert, H. Walcher, R. Kohl, N. Herres, R. Locher, R. Samlenski, R. Brenn, Diamond Relat. Mater. 2 (1993) 158.
[12] R. Locher , C. Wild, N. Herres, D. Behr, P. Koidl, Appl. Phys. Lett. 65 (1994) 34.
[13] A.F. Wells, Philos. Mag. 37 (1946) 605.
[14] W.B. Alexander, P.H. Holloway, L. Heatherly, R.E. Clausing, Surf. Coat. Technol. 45/55 (1992) 387.
[15] Z. Yu, A. Flodström, Surf. Sci. 401 (1998) 236.
[16] Y. Sato, M. Kamo, Surf. Coat. Technol. 39/40 (1989) 183.
[17] K. Kobashi, K. Nishimura, K. Miyata, K. Kumagai, A. Nakaue, J. Mater. Res. 5 (1990) 2469.
[18] M.A. Tamor, M.P. Everson, in: C.L. Renschler, D.C. Pouch, Y. Achiba (Eds.), Mater. Res. Soc. Symp. Proc., Vol. 349, MRS, Pittsburgh, PA, 1994, p. 391.
[19] S. Jin, T. Moustakas, Appl. Phys. Lett. 65 (1994) 403.
[20] N. Lee, A. Badzian, Appl. Phys. Lett. 67 (1995) 2011.

[21] M. Marinelli, A. Hatta, T. Ito, A. Hiraki, T. Nishino, Appl. Phys. Lett. 68 (1996) 1631.
[22] B.V. Spitsyn, L.L. Bouilov, B.V. Derjaguin, J. Cryst. Growth 52 (1981) 219.
[23] K. Kobashi, K. Nishimura, Y. Kawade, T. Horuchi, Phys. Rev. B 38 (1988) 4067.
[24] R.E. Clausing, L. Heatherly, K.L. More, G.M. Begun, Surf. Coat. Technol. 39/40 (1989) 199.
[25] Y.-J. Baik, K.Y. Eun, Thin Solid Films 212 (1992) 156.
[26] M.A. Tamor, M.P. Everson, J. Mater. Res. 9 (1994) 1839.
[27] J.L. Kaae, P.K. Gentzel, J. Chin, W.P. West, J. Mater. Res. 5 (1990) 1480.
[28] D.R. Lide, H.P.R. Frederikse (Eds.), CRC Handbook of Chemistry and Physics, CRC Press, Boca Raton, FL, 77th ed., 1996.
[29] W.-M. Sebert, E. Wörner, F. Fuchs, C. Wild, P. Koidl, Appl. Phys. Lett. 63 (1996) 759.
[30] M. Moore, Ind. Diamond Rev. 2 (1985) 67.
[31] M.A. Tamor, M.P. Everson, J. Mater. Res. 9 (1994) 1839.
[32] F.C. Frank, in: Doremus, Roberts, Turnbull (Eds.), Growth and Perfection of Crystals, Wiley, New York, 1958, p. 3.
[33] R. Kern, in: I. Sunagawa (Ed.), Morphology of Crystals, Terra, Tokyo, 1987, pp. 79–206.
[34] C. Herring, Phys. Rev. 82 (1951) 87.
[35] P. Hartman, W.G. Perdok, Acta Crystallogr. 8 (1955) 49.
[36] P. Hartman, W.G. Perdok, Acta Crystallogr. 8 (1955) 512.
[37] P. Hartman, W.G. Perdok, Acta Crystallogr. 8 (1955) 525.
[38] P. Hartman, in: I. Sunagawa (Ed.), Morphology of Crystals, Terra, Tokyo, 1987, pp. 269–319.
[39] M. Frenklach, H. Wang, Phys. Rev. B 42 (1991) 1520.
[40] M. McEllistrem, M. Allgeier, J.J. Boland, Sience 279 (1998) 545.
[41] R.E. Thomas, R.A. Rudder, R.J. Markunas, J. Vac. Sci. Technol. A 10 (1992) 2451.
[42] R. Samlenski, C. Haug, R. Brenn, Appl. Phys. Lett. 67 (1995) 2798.
[43] A. van der Drift, Philips Res. Rep. 22 (1967) 267.